References and Notes

1. J. B. Kortright *et al.*, *J. Magn. Magn. Mater.* **207**, 7 (1999).
2. G. A. Prinz, *Science* **282**, 1660 (1998).
3. For a recent review, see J. Nogues and I. K. Schuller, *J. Magn. Magn. Mater.* **192**, 203 (1999).
4. H. A. Dürr *et al.*, *Science* **284**, 2166 (1999).
5. A. Scholl *et al.*, *Science* **287**, 1014 (2000).
6. S. Blügel, M. Weinert, P. H. Dederichs, *Phys. Rev. Lett.* **60**, 1077 (1988).
7. C. Krembel, M. C. Hanf, J. C. Peruchetti, D. Bolmont, G. Gewinner, *J. Magn. Magn. Mater.* **93**, 529 (1991).
8. P. Hohenberg and W. Kohn, *Phys. Rev. B* **136**, 864 (1964).
9. We used the density functional theory method, which is first-principles in that it requires no experimental input other than the nuclear charges. The FLAPW method is among the most accurate electronic structure methods, assuming no shape approximation to the charge density or potential. It is ideally suited to the problem of transition-metals in open geometry such as surfaces. Further, we use a film method with a semi-infinite vacuum, which provides a numerically excellent representation of states participating in the tunneling. No sensitivity of our results was found with respect to our choice of computational parameters, such as the number of $\mathbf{k}_{\|}$ (reciprocal lattice points used in 2D Brillouin-zone integrals) or basis-set sizes.
10. V. L. Moruzzi, J. F. Janak, A. R. Williams, *Calculated Electronic Properties of Metals* (Pergamon, New York, 1978).
11. R. Wiesendanger *et al.*, *Phys. Rev. Lett.* **65**, 247 (1990).
12. R. Wiesendanger *et al.*, *Science* **255**, 583 (1992).
13. S. Heinze, S. Blügel, R. Pascal, M. Bode, R. Wiesendanger, *Phys. Rev. B* **58**, 16432 (1998).
14. J. Tersoff and D. R. Hamann, *Phys. Rev. Lett.* **50**, 1998 (1983).
15. V. P. LaBella *et al.*, *Phys. Rev. Lett.* **83**, 2989 (1999).
16. S. Heinze, R. Abt, S. Blügel, G. Gilarowski, H. Niehus, *Phys. Rev. Lett.* **83**, 4808 (1999).
17. O. Pietzsch, A. Kubetzka, D. Haude, M. Bode, R. Wiesendanger, *Rev. Sci. Instrum.* **71**, 424 (2000).
18. M. Bode, M. Hennefarth, D. Haude, M. Getzlaff, R. Wiesendanger, *Surf. Sci.* **432**, 8 (1999).
19. A better quantitive agreement can be obtained by including more localized tip-orbitals such as d_{z^2}, whose corrugation amplitudes are much closer to the experiment in (*13*).
20. M. Bode, M. Getzlaff, R. Wiesendanger, *Phys. Rev. Lett.* **81**, 4256 (1998); *J. Vac. Sci. Technol. A* **17**, 2228 (1999).
21. In the calculation, we assumed the magnetization axes of the sample and the probe tip to be collinear, i.e., $\cos\theta = \pm 1$, and a spin-polarization of the tip states $P_T = 0.4$. This value has been determined in earlier experiments (*20*). In the present experimental setup, the degree of alignment cannot be controlled and, in principle, it can be noncollinear, which might explain the discrepency between theory and experiment.
22. The in-plane or out-of-plane magnetization direction of tips coated by thin films is governed by the interface and surface anisotropy of the film material, i.e., Fe or Gd, in contact with the most densely packed W surface, i.e., W(110), which is formed at the tip apex after the thermal flash. To our experience, slight deviations from the ideal magnetization directions were frequently observed, probably caused by the local atom morphology of the tip.
23. O. Pietzsch, A. Kubetzka, M. Bode, R. Wiesendanger, *Phys. Rev. Lett.* **84**, 5212 (2000).

24. Financial support from the Deutsche Forschungsgemeinschaft (grant Wi 1277/6 and Bl 444/1-1), from the German-Israeli Foundaiton (grant I-550-184.14/97), and from the Bundesministerium für Bildung und Forschung (grant 13N7647) is gratefully acknowledged.

29 February 2000; accepted 25 April 2000

A Nanoplotter with Both Parallel and Serial Writing Capabilities

Seunghun Hong and Chad A. Mirkin*

The development of an eight-pen nanoplotter capable of doing parallel dip-pen nanolithography (DPN) is reported. Because line width and patterning speed in DPN are independent of contact force, only one of the tips in the parallel writing mode (the "imaging" tip) has a feedback system to monitor tip position and to write the pattern; all other tips reproduce what occurs at the imaging tip in a passive fashion. Proof-of-concept experiments that demonstrate eight-pen parallel writing, ink and rinsing wells, and "molecular corralling" via a nanoplotter-generated structure are reported.

The greatest limitation in using scanning-probe methodologies for doing ultrahigh-resolution nanolithography over large areas derives from the serial nature of most of these techniques. For this reason, scanning probe lithography (SPL) methods have been primarily used as customization tools for preparing and studying academic curiosities (*1–9*). If SPL methodologies are ever to compete with optical or even stamping lithographic methods for patterning large areas (*10–12*), they must be expanded to parallel processes. Several important steps have been taken in this direction. For example, researchers have developed a variety of different multiple-probe instruments for scanning (*13–16*), and some have begun to use these instruments for parallel SPL. In particular, Quate and coworkers have shown that as many as 50 tips can be used at once (*15*), and with such a strategy, both imaging and patterning speeds could be dramatically improved. However, a major limitation of all parallel SPL methods thus far developed is that each tip within the array needs a separate feedback system, which dramatically increases the instrumentation complexity and cost. One of the reasons separate feedback systems are required in such processes is that tip-substrate contact forces influence the line width and quality of the patterned structures. Although parallel scanning tunneling microscope lithography has not yet been demonstrated, such a process would presumably require a feedback system for each tip that would allow one to maintain constant tunneling currents. Herein, we report a method for doing parallel or single-pen soft nanolithography using an array of cantilevers and a conventional atomic force microscope (AFM) with a single feedback system.

Recently, we invented a type of serial SPL, called dip-pen nanolithography (DPN) (*17–20*), in which organic molecules ("inks"), which are cast onto an AFM tip, are deposited through a water meniscus (*21*) directly onto an underlying substrate. An ink that reacts with the substrate is often chosen so that the process will yield stable monolayer structures. The technique can be applied in general with many types of molecule-based inks (*17–20*), it works under ambient conditions, it offers 15-nm line-width resolution and 5-nm spatial resolution, and it can be done over relatively large areas in automated fashion. Moreover, others have shown that DPN can be merged with nanografting to increase the resolution of this lithography further for soft structures (*22*). However, as with most other SPL methods, DPN thus far has been used exclusively in a serial format. Finally, it is important to note that others have unsuccessfully attempted to use scanning-probe instruments to transport organic materials onto solid substrates to form stable nanostructures (*23*). It is, in part, the recognition of the existence of the meniscus (*21*) and the ability to use it as an ink transport medium under regulated humidity (*17–20*) that make controlled molecular writing on the nanometer-length scale possible.

All experiments were performed on a Thermomicroscopes M5 AFM, which is equipped with a closed-loop scanner that minimizes thermal drift. Custom nanolithography software was used to drive the instrument. The instrument has a 200-mm by 200-mm sample holder mounted on an automated translation stage. The details of serial, single-tip DPN writing and pattern alignment procedures have been described elsewhere (*19*). Our intention in transforming DPN into a parallel process was to create an SPL method that enables one to generate multiple, single-

Department of Chemistry and Northwestern University Center for Nanofabrication and Molecular Self-Assembly, Northwestern University, 2145 Sheridan Road, Evanston, IL 60208, USA.

*To whom correspondence should be addressed. E-mail: camirkin@chem.nwu.edu

ink patterns in parallel or a single multiple-ink pattern in series. This tool would be the nanotechnologist's equivalent of a multiple-pen nanoplotter with parallel writing capabilities. To accomplish this goal, several modifications of the AFM and DPN process were required (Scheme 1). First, ink wells were fabricated for addressing and inking the pens individually in our nanoplotter. Specifically, we have found that rectangular pieces of filter paper soaked with different inks or solvents can be used as ink wells and rinsing wells, respectively, and can be located at the periphery of the sample to be patterned. An AFM tip can be coated with a molecular ink or solvent of interest simply by making contact with the appropriate filter paper–based ink or rinsing well for 30 s (contact force = 1 nN). Both inking and rinsing procedures are automated by custom software, which drives the X-Y-Z translation stage. Second, a tilt stage (purchased from Newport Corporation, sensitivity ~10 μrad) was added to the AFM that enables one to control orientation of the sample with respect to the ink-coated tips; this allows one to selectively engage single or multiple tips during a patterning experiment (Scheme 1). Finally, a multiple-tip array was fabricated simply by physically separating an array of cantilevers from a commercially available wafer block containing 250 individual cantilevers (Thermomicroscopes Sharpened Microlevers C, force constant = 0.01 N/m) and then using that array as a single cantilever (*24*). The array is affixed to a ceramic tip carrier that comes with the commercially acquired mounted cantilevers.

A key scientific observation allows DPN to be transformed from a serial to parallel process without substantially complicating the instrumentation required to do DPN. Features (for example, dots and lines) generated from inks such as 1-octadecanethiol (ODT), under different contact forces that span a range of two orders of magnitude, are virtually identical with respect to diameter and line width. We found it surprising that patterning experiments conducted with even a small negative contact force, where the AFM tip bends down to the surface, exhibit ink transport rates that are comparable to experiments executed with the tip-substrate contact force as large as 4 nN (Fig. 1). Thus, in DPN writing, the ink molecules migrate from the tip through the meniscus to the substrate by diffusion, and the tip is simply acting as a point source for molecular flow.

In a typical parallel, multiple-pen experiment involving a cantilever array, each tip is coated with an ink by dipping it into the appropriate ink well. For the sake of simplicity, we initially describe experiments involving only two cantilevers in the array. One tip, designated "the imaging tip," is used for both imaging and writing; the second tip is used simply for writing. The imaging tip is used the way a normal AFM tip is used and is interfaced with force sensors providing feedback; the writing tips do not need feedback systems. In a patterning experiment, the imaging tip is used to determine overall surface topology, to locate alignment marks generated by DPN, and to pattern molecules lithographically in an area with coordinates defined with respect to the alignment marks (*19*). With this strategy, the writing tip(s) reproduce the structure generated with the imaging tip at a distance determined by the spacing of the tips in the cantilever array (600 μm in the case of a two-pen experiment).

To begin parallel patterning, the tilt stage is adjusted so that the writing tip is 0.4 μm closer to the sample than the imaging tip. The tip-to-sample distances in an array experiment can be monitored with the Z-stepper motor counter. The laser is placed on the imaging tip so that during patterning both tips are in contact with the surface (Scheme 1). For the first demonstration of parallel writing, we coated two tips with the same ink, ODT (Fig. 2A). In this experiment, two one-molecule-thick nanostructures made of ODT are patterned onto a gold surface by moving the imaging tip along the surface in the form of a square (contact force ~0.1 nN; relative humidity ~30%; writing speed = 0.6 μm/s).

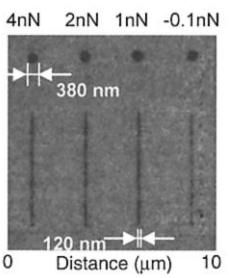

Fig. 1. Lateral force microscopy (LFM) images of ODT monolayer nanodot and line features on gold generated by the same tip but under different tip-substrate contact forces. Feature sizes vary less than 10%.

Note that the line widths are nearly identical, and the nanostructure registration (orientation of the first square with respect to the second) is near perfect (less than 2 mrad angle variation). Parallel patterning can be accomplished with more than one ink. In this case, the imaging tip, attached to the instrument, is placed in a rinsing well to remove the ODT ink and then coated with 16-mercaptohexadecanoic acid (MHA) by immersing it in an MHA ink well. The parallel multiple-ink experiment is then carried out in a manner analogous to the parallel single-ink experiment (contact force ~0.1 nN; relative humidity ~30%; writing speed = 0.4 μm/s). The two resulting nanostructures can be differentiated when viewed with a lateral force microscope but, again, are perfectly aligned

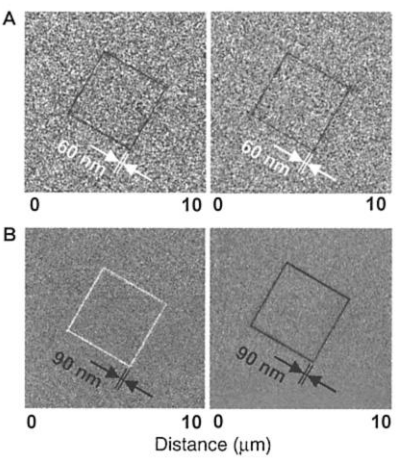

Fig. 2. Parallel DPN writing using two tips and a single feedback system. (**A**) Two nearly identical ODT patterns generated on gold in parallel fashion with a two-pen cantilever. (**B**) Two nearly identical patterns generated on gold in parallel fashion with a two-pen cantilever with each pen coated with a different ink. The pattern on the left was generated from an MHA-coated tip and exhibits a higher lateral force than the gold substrate. The pattern on the right was generated with an ODT-coated tip and exhibits a lower lateral force than the gold substrate.

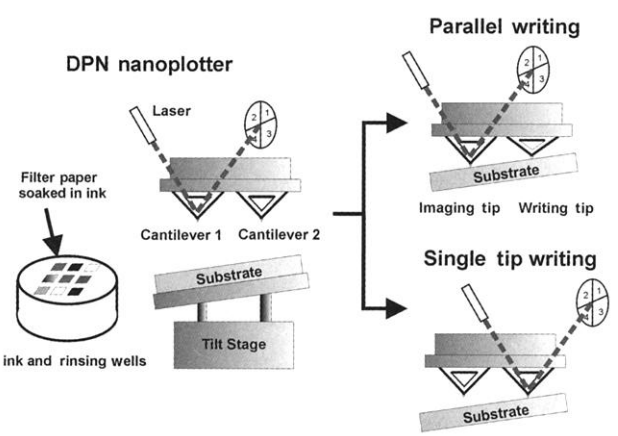

Scheme 1.

because of the rigid, fixed nature of the two tips (Fig. 2B). Note that the line widths of the two patterns are identical to within 15%. This level of reproducibility likely is a coincidental result, because feature size and line width in a DPN experiment often depend on the transport properties of the specific inks (for example, solubility) and ink loading (for example, ink coating thickness and residual solvent).

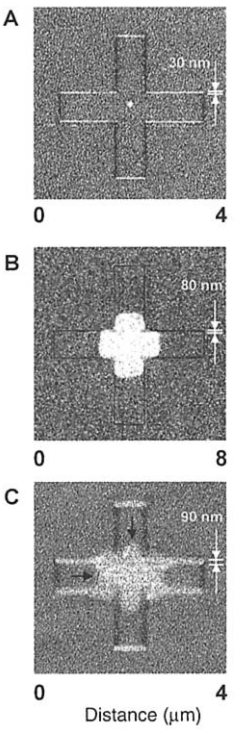

Fig. 3. LFM images of nanoplotter-generated monolayer patterns, which consist of features composed of two different inks, ODT (dark grey) and MHA (white). The patterns were generated without removing the multiple-pen cantilever from the instrument. (**A**) Two ink, cross-shaped pattern with an MHA dot in the center of the pattern; note the circular shape of the dot. (**B**) A molecular cross-shaped corral made of ODT. The MHA molecules diffuse from the center of the corral but are blocked when they reach the 80-nm-wide ODT walls. Note the convex shape of the MHA ink within the molecular corral attributable to the different wetting properties of the gold substrate and hydrophobic corral. (**C**) A molecular cross-shaped corral, where the horizontal lines are composed of MHA and the vertical lines are comprised of ODT. Note that the MHA, which was introduced in the center of the corral diffuses over the walls of the corral made of MHA but remains confined within the walls made of ODT. Also, note that the MHA structure within the corral assumes a concave shape where the side walls are made of MHA (horizontal black arrow) and a convex shape where the side walls are made of ODT (vertical black arrow).

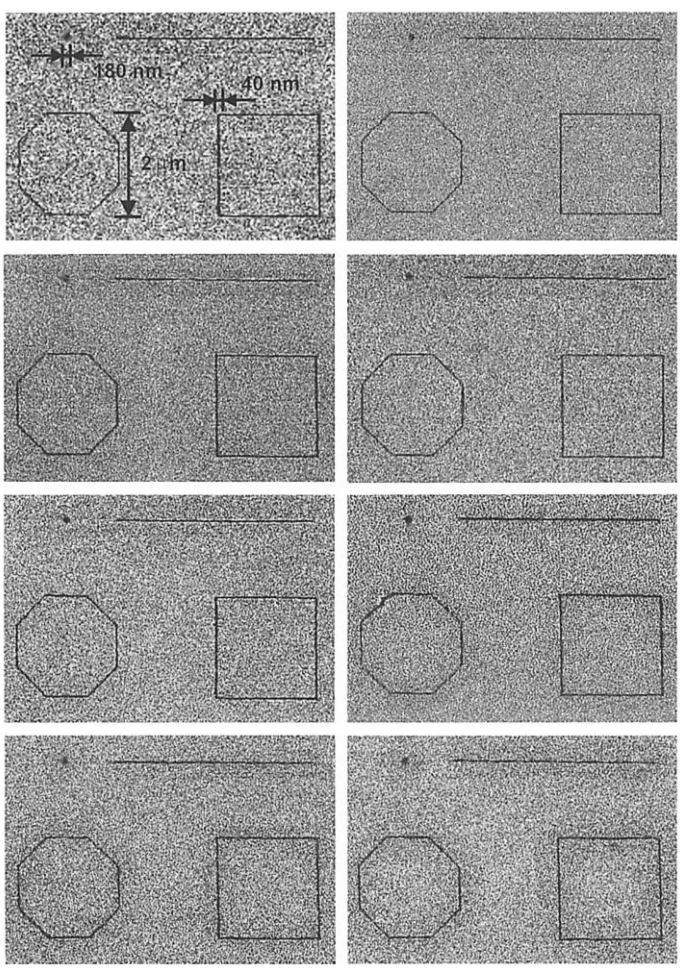

Fig. 4. LFM images of eight identical patterns generated with one imaging tip and eight writing tips coated with ODT molecules.

A remarkable feature of this type of nanoplotter is that the system also can be operated in serial fashion to generate customized nanostructures made of different inks. To demonstrate this capability, we used a cantilever array that had a tip coated with ODT and a tip coated with MHA. The laser was focused on the ODT-coated tip, and the tilt stage was adjusted so that only this tip was in contact with the surface (Scheme 1). The ODT-coated tip was then used to generate the vertical sides of a cross on a gold surface (contact force ~0.1 nN; relative humidity ~30%; writing speed = 1.3 μm/s) (Fig. 3A). The laser was then moved to the MHA-coated tip, and the tilt stage was readjusted so that only this tip was in contact with surface. The MHA tip was then used to draw the 30-nm-wide horizontal sides of the nanostructure ("nano" refers to line width) (Fig. 3A). Microscopic ODT alignment marks deposited on the periphery of the area to be patterned are used to locate the initial nanostructure as described elsewhere (*19*).

This type of multiple-ink nanostructure with a bare gold interior would be difficult, if not impossible, to prepare via stamping methodologies or conventional nanolithography methods but was prepared in 5 min with the automated multiple-pen nanoplotter described here. Moreover, this tool and these types of structures can now be used for evaluating important issues of adsorbate diffusion (*25*) on the nanometer-length scale and across nanoscale, one-molecule-thick barriers. As a proof-of-concept, we examined the diffusion of MHA from a tip to the surface within this type of "molecule-based corral." As a first step, a cross shape was generated with a single-ink, ODT-coated tip (contact force ~0.1 nN; relative humidity ~30%; writing speed = 0.5 μm/s). Then, an MHA-coated tip was held in contact with the surface for 10 min (contact force ~0.1 nV) at the center of the cross so that MHA molecules were transported onto the surface and could diffuse out from the point of contact. Even 80-nm-wide ODT lines act as a diffusion barrier, and MHA molecules are trapped inside the ODT cross pattern (Fig. 3B). When the horizontal sides of the molecular corral are made of MHA barriers, the MHA molecules diffuse from the tip onto the surface and over the hydrophilic MHA barriers. It is noteworthy that in this two-component nanostructure, the MHA does not go over the ODT barriers, resulting in an anisotropic pattern (Fig. 3C). Although we do not yet know whether the corral is changing the shape of the meniscus, which in turn controls ink diffusion, or alternatively, the ink is deposited and then mi-

grates from the point of contact to generate this structure, this type of proof-of-concept experiment is a first step toward discovering and studying important interfacial processes with this new nanotechnology tool.

The parallel nanoplotting strategy reported here is not limited to two tips. Indeed, we have shown that a cantilever array consisting of eight tips can be used to generate nanostructures in parallel fashion. In this case, each of the eight tips are coated with ODT. The outermost tip is designated as the imaging tip, and the feedback laser is focused on it during the writing experiment. To demonstrate this concept, we generated four separate nanostructures, a 180-nm dot (contact force ~0.1 nN, relative humidity = 26%, contact time = 1 s), a 40-nm-wide line, a square, and an octagon (contact force ~0.1 nN, relative humidity ~26%, writing speed = 0.5 μm/s), and we reproduced these structures in parallel fashion with the seven passively following tips (Fig. 4). Note that there is a less than 10% standard deviation in line width for the original nanostructures and the seven copies.

The number of pens that can be used in a parallel DPN experiment to reproduce nanostructures passively is not limited to eight. Indeed, there is no reason why the number of pens cannot be increased to hundreds or even a thousand pens without the need for additional feedback systems. Finally, this work opens avenues for researchers to begin using DPN and conventional AFM instrumentation to do high-resolution and aligned patterning of nanostructures on a large scale that is automated and moderately fast.

References and Notes

1. E. S. Snow, P. M. Campbell, F. K. Perkins, *Appl. Phys. Lett.* **75**, 1476 (1999).
2. R. Luthi *et al.*, *Appl. Phys. Lett.* **75**, 1314 (1999).
3. L. A. Bottomley, *Anal. Chem.* **70**, 425R (1998).
4. J. K. Schoer and R. M. Crooks, *Langmuir* **13**, 2323 (1997).
5. S. Xu and G. Y. Liu, *Langmuir* **13**, 127 (1997).
6. R. M. Nyffenegger and R. M. Penner, *Chem. Rev.* **97**, 1195 (1997).
7. H. Sugimura and N. Nakagiri, *J. Vac. Sci. Technol. A* **14**, 1223 (1996).
8. H. U. Muller, C. David, B. Volkel, M. Grunze, *J. Vac. Sci. Technol. B* **13**, 2846 (1995).
9. Y. Kim and C. M. Lieber, *Science* **257**, 375 (1992).
10. Y. Xia, J. A. Rogers, K. E. Paul, G. M. Whitesides, *Chem. Rev.* **99**, 1823 (1999).
11. R. J. Jackman, J. L. Wilbur, G. M. Whitesides, *Science* **269**, 664 (1995).
12. S. Y. Chou, P. R. Krauss, P. J. Renstrom, *Appl. Phys. Lett.* **67**, 3114 (1995).
13. M. Lutwyche *et al.*, *Sens. Actuators A* **73**, 89 (1999).
14. P. Vettiger *et al.*, *Microelectron. Eng.* **46**, 11 (1999).
15. S. C. Minne *et al.*, *Appl. Phys. Lett.* **73**, 1742 (1998).
16. S. Tsukamoto, B. Siu, N. Nakagiri, *Rev. Sci. Instrum.* **62**, 1767 (1991).
17. R. D. Piner, J. Zhu, F. Xu, S. Hong, C. A. Mirkin, *Science* **283**, 661 (1999).
18. S. Hong, J. Zhu, C. A. Mirkin, *Langmuir* **15**, 7897 (1999).
19. ———, *Science* **286**, 523 (1999).
20. C. A. Mirkin, *MRS Bull.* **2000**, 43 (January 2000).
21. R. D. Piner and C. A. Mirkin, *Langmuir* **13**, 6864 (1997).
22. N. A. Amro, S. X. Xu, G. Y. Liu, *Langmuir* **16**, 3006 (2000).
23. M. Jaschke and H. J. Butt, *Langmuir* **11**, 1061 (1995).
24. Supplementary material is available at www.sciencemag.org/feature/data/1050099.shl.
25. E. Delamarche *et al.*, *J. Phys. Chem. B* **102**, 3324 (1998).

26. This work was supported by the Air Force Office of Scientific Research, the Defense Advanced Research Projects Agency, and the NSF-funded Northwestern University Materials Research Center. P. V. Schwartz is acknowledged for helpful discussions.

3 March 2000; accepted 27 April 2000

Electronic Structure of Mott Insulators Studied by Inelastic X-ray Scattering

M. Z. Hasan,[1]* E. D. Isaacs,[2] Z.-X. Shen,[1] L. L. Miller,[3] K. Tsutsui,[4] T. Tohyama,[4] S. Maekawa[4]

The electronic structure of Mott insulators continues to be a major unsolved problem in physics despite more than 50 years of research. Well-developed momentum-resolved spectroscopies such as photoemission or neutron scattering cannot probe the full Mott gap. High-resolution resonant inelastic x-ray scattering revealed dispersive charge excitations across the Mott gap in a high–critical temperature parent cuprate ($Ca_2CuO_2Cl_2$), shedding light on the anisotropy of the Mott gap. These charge excitations across the Mott gap can be described within the framework of the Hubbard model.

The discovery of high–critical temperature (T_c) superconductivity and colossal magnetoresistance in doped transition metal oxides has led to extensive research interest in Mott insulators. Such oxides are characterized by large onsite Coulomb interaction and theconsequent low-temperature insulating state characterized by a charge excitation gap, known as the Mott gap. The gap is either set by the Coulomb interaction U or the charge transfer energy Δ (energy to remove an electron from the oxygen orbital and put it on the copper site), depending on which one is lower (*1–4*). Angle-resolved photoemission spectroscopy (ARPES), which probes only the occupied electronic states, has been remarkably successful in characterizing the electronic structure of cuprate-based insulators (*5–8*). Little is known about the momentum- resolved (**k**-resolved) electronic structure of the unoccupied band, which is a major barrier for a coherent understanding of the nature of the Mott gap and its related insulating state. In addition, knowledge of the unoccupied upper Hubbard band (UHB) is essential to understand the physics of n-type (electron-doped) superconductors, as the doped electrons occupy the UHB. Among the standard probes of condensed matter systems (which allow momentum-resolved studies), neutrons do not couple to electrons' charge density, and (thermal) neutron energy is too low to reach the Mott edge. No **k**-resolved inverse photoemission (Inv-ARPES) study is available because of problems associated with sample charging as well as the lack of required energy resolution. Inelastic electron scattering, also known as electron energy-loss spectroscopy (EELS), measures electronic excitations from the occupied to the unoccupied bands; however, EELS requires extensive sample preparation and does not yield useful information unless the spectra are corrected for multiple scattering effects (*9*).

Inelastic x-ray scattering is a natural and powerful probe of electronic excitations in condensed matter systems. It has the potential to improve our understanding of the bulk electronic structure of correlated electron systems. Inelastic scattering of x-ray photons covers a fairly wide kinematic range in energy and momentum space, and the photons directly couple to the electronic charge (and to other electronic degrees of freedom, such as orbitals and spins). However, because x-ray photons are highly absorbed in high-Z materials (where Z is the atomic number), applications of the technique have been mostly limited to low-Z systems (*10–13*). Recent experimental results and theoretical/numerical investigations have shown that by tuning the incident photon energy near an x-ray absorption edge, a Raman-like effect can be measured with nonzero momentum transfer (despite the high absorption cross section) through the large resonant enhancement, which eventually dominates the overall cross section (*14–19*). An inelastically scattered x-ray photon can probe the full charge

[1]Department of Applied Physics, Stanford Synchrotron Radiation Laboratory (SSRL), and Stanford Linear Accelerator Center (SLAC), Stanford University, Stanford, CA 94305, USA. [2]Bell Laboratories, Lucent Technologies, Murray Hill, NJ 07974, USA. [3]Department of Physics and Ames Laboratory, Iowa State University, Ames, IA 50011, USA. [4]Institute of Materials Research, Tohoku University, Sendai 980-8577, Japan.

*To whom correspondence should be addressed. E-mail: mzhasan@stanford.edu